RESEARCH ARTICLE

Key Points:
- Rainfall rates over different zones are distinctive between strong and weak ISMRs
- Rainfall rates over NEI show insensitivity to the strength of ISMRs
- Greater likelihood of moderate versus light daily rainfall rate causes larger rainfall during strong versus weak monsoons

Correspondence to:
Y. Zheng,
yzheng@fsu.edu

Distinctive features of rainfall over the Indian homogeneous rainfall regions between strong and weak Indian summer monsoons

Yangxing Zheng[1], M. A. Bourassa[1,2], M. M. Ali[1], and T. N. Krishnamurti[2]

[1]Center for Ocean-Atmospheric Prediction Studies, Florida State University, Tallahassee, Florida, USA, [2]Department of Earth, Ocean, Atmospheric Science, Florida State University, Tallahassee, Florida, USA

Abstract Studies of Indian summer monsoon rainfall (ISMR: June–September) on regional scales are critically important for various applications related to agriculture and water management in India. Based on the coherent rainfall over regional scales, the India Meteorological Department defined four so-called homogeneous regions: northwest India (NWI), northeast India (NEI), central India (CI), and south peninsula India (SPIN). Here we present the salient features of daily rainfall behavior over these four regions and their association with the strength of ISMRs between strong and weak monsoons. Our results reveal that rainfall rates are primarily stronger (weaker) over NWI, CI, and SPIN during strong (weak) monsoons, while rainfall rates over NEI show no remarkable changes between strong and weak monsoons. Specifically, stronger rainfalls over NWI, CI, and SPIN during strong monsoons are generally caused by prolonged and strong wet spells followed by short and weak dry spells, primarily during the mature phase and the withdrawal phase. In contrast, weaker rainfalls over NWI, CI, and SPIN during weak monsoons are mainly caused by the prolonged and strong dry spells, which mostly occur in July–August, followed by short wet spells. The distinctive rainfall features over each region are closely associated with the characteristics of regional convective activity over each region. The rainfall rates over NEI appear insensitive to the strength of ISMRs. Finally, a probability density function analysis indicates that the rainfall rates over the four homogeneous regions between strong and weak monsoons can be characterized by the likelihood of occurrence of different rainfall ranges.

1. Introduction

The success or failure of Indian summer monsoon rainfall (ISMR) has profound impacts on Indian agriculture and food production. Several previous studies [*Kumar et al.*, 2006; *Annamalai et al.*, 2013] have used the summer rainfalls that are averaged over the entire Indian region as one unit (all-India rainfall, i.e., AIR) to represent a measure of the strength of ISMR, which is a weighted average of the June–September (JJAS) rainfall at 306 well-distributed rainfall gauge stations across India [*Parthasarathy et al.*, 1992, 1994, 1995]. However, the ISMR over different regions is known to have considerable variability at different temporal scales [*Ramamurthy*, 1969; *Thapliyal and Kulshrestha*, 1991; *Gadgil et al.*, 1993; *Iyengar and Basak*, 1994; *De et al.*, 1998; *Krishnamurthy and Shukla*, 2000; *Kripalani and Kulkarni*, 2001; *Dash et al.*, 2002; *Kripalani et al.*, 2003; *Sahai et al.*, 2003; *Gadgil*, 2003; *Goswami*, 2005; *Rao et al.*, 2009; *Malik et al.*, 2010; *Rajeevan et al.*, 2010; *Kulkarni et al.*, 2011]. For instance, *Gadgil et al.* [1993] found that the JJAS rainfall does not change coherently at 200 stations across India. *Dash et al.* [2002] reported that the spatial variations of rainfall vary from 8.5% in the northeast India (NEI) to 27% in the northwest India (NWI). While some portions of the country receive excess rainfall, other sectors experience severe droughts. These previous studies suggest that ISMR exhibits complex variability in time and space. Therefore, the AIR index may not be useful for various applications such as those related to regional agriculture and water management.

Meanwhile, early observational studies [*Gadgil et al.*, 1993; *Iyengar and Basak*, 1994] have revealed that rainfall can be coherent in space over smaller spatial scales (~100 km). The homogeneous feature of rainfall over regional scales allows for practical regional water management applications. To determine the temporal and spatial variability of rainfall on a regional scale, it is useful to analyze the rainfall averaged over a homogeneous region rather than average the rainfall at all individual stations within that region. Doing so reduces small-scale variability and enhances signal variation for regional forecasts [*Nicholson*, 1986]. Additionally, in order to improve rainfall prediction across smaller regions it is necessary to define a homogeneous rainfall region. With this in mind, the India Meteorology Department (IMD) defined four homogeneous rainfall regions of the Indian
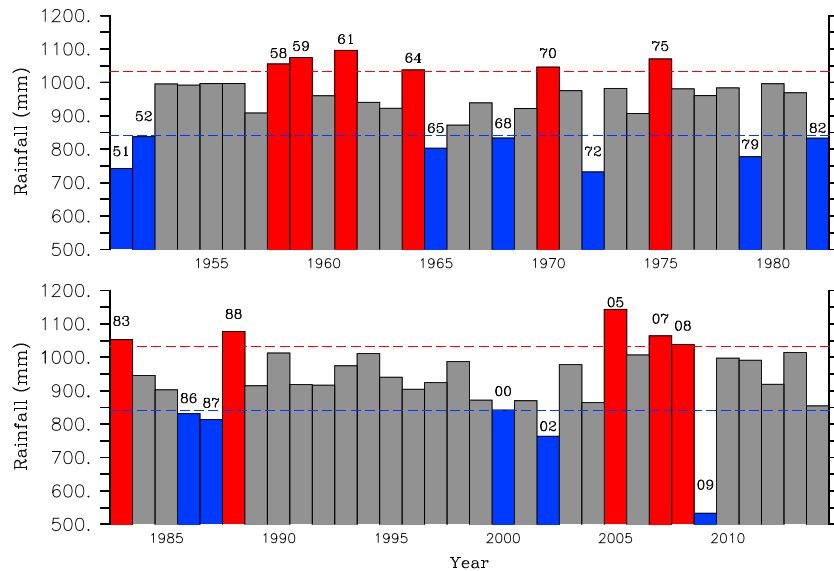
Figure 1. Evolution of JJAS Indian rainfall (in mm) over the period 1951–2014 derived from the daily gridded rainfall product provided by IMD. Strong (red bars), weak (blue bars), and normal (gray bars) ISMRs are identified by the departure of JJAS rainfall of each year from the JJAS rainfall climatology computed over the period 1951–2014, whose departure values are larger than +10%, smaller than −10%, and within −10% and 10% of the seasonal climatology, respectively. The red (blue) dashed line denotes a value of 110% (90%) of seasonal climatology (i.e., the mean climatology is 937.7 mm), which is 1031 mm (844 mm). The years of strong and weak ISMRs are denoted by the numbers over the bars.

subcontinent: northwest India (NWI), northeast India (NEI), central India (CI), and south peninsula (SPIN). Hereafter, we refer to these four regions as the IMD regions. These regions were selected for our study based on meteorological records (prepared on the basis of 306 fixed well-distributed rain gauges in the plain regions of India), which show that the variation in rainfall over substantial portions of each of the meteorological subdivisions that make up the region is positively and significantly correlated with the area-weighted rainfall variation over the region as a whole [*Parthasarathy et al.*, 1995]. Furthermore, the IMD produced a seasonal rainfall series for the four regions over the period 1901–2013. Some caution must be taken with this interpretation: strong correlations ensure proportionality rather than similarity in magnitude. For example, the rainfall magnitude is much greater in the western SPIN region than in the eastern part of the region. Researchers such as *Pattanaik* [2007a, 2007b] have also used the IMD regions for analysis. *Pattanaik* [2007a] examined rainfall variability over these four regions of India in relation to the variability in westward movement frequency of monsoon depressions, and *Pattanaik* [2007b] used rainfall over the regions to discuss the association with variability of convective activity over the northern Indian Ocean. Most recently, *Zheng et al.* [2016] suggested that the rainfall in NWI, CI, and SPIN characterizes whether an ISMR is strong or weak. Although rainfall inhomogeneity across India has been studied, some important questions remain unanswered. For example, are the rainfall features in these four homogeneous rainfall zones significantly different under strong and weak Indian summer monsoon regimes, particularly at short time scales (e.g., several days, synoptic scales)? And if such differences exist, what are the potential mechanisms leading to the differences? Determining this would help improve India's regional rainfall forecasts during Indian summer monsoon periods. Therefore, the primary purpose of this work is to address the above questions, utilizing the most recent daily gridded rainfall data sets over the period 1951–2014 released by IMD.

The remainder of this paper is organized as follows. The data sets and methods used in this study are described in section 2. Section 3 defines strong, weak, and normal ISMRs over the period 1951–2014 and delineates the evolution of rainfall anomalies over the four homogeneous regions during the summer monsoon season of each strong and weak ISMR year. An emphasis is placed upon characteristics of above normal/below normal conditions (i.e., wet/dry spells) over each homogeneous region for strong and weak ISMRs. Section 4 provides potential linkages between rainfall over the four homogeneous regions and the total ISMR. Section 5 presents salient features of the probability density function (PDF) of daily rainfall distribution during strong, weak, and normal monsoon seasons over the four homogeneous regions, showing that there are substantial shifts in
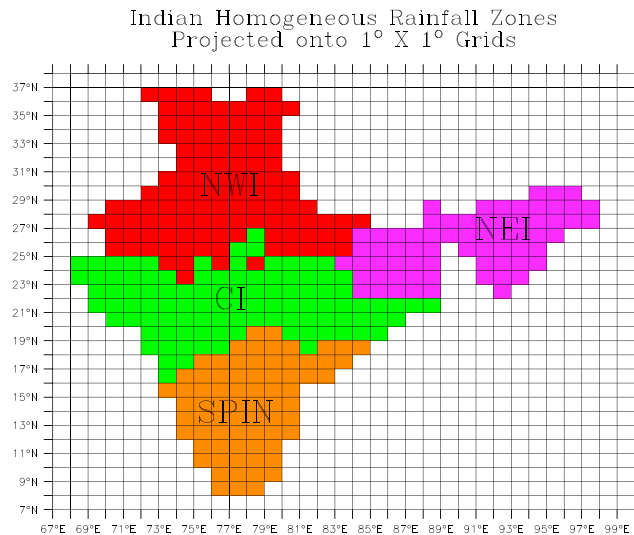
Figure 2. Map of the four Indian homogeneous rainfall zones projected onto $1^\circ \times 1^\circ$ daily rainfall grids. NWI, CI, SPIN, and NEI are shown in red, green, orange, and purple, respectively.

the PDFs. Some potential hypotheses for distinctive features of rainfall rate over the four homogeneous regions are discussed in section 6. One clear finding is that the PDFs for deep convection are consistent with the PDFs for rain rate, indicating that changes in monsoon rainfall rate are linked to changes in deep convection.

2. Data and Methods

2.1. Daily Rainfall Data and Geostationary IR Channel Brightness Temperature

This study used the latest daily $1^\circ \times 1^\circ$ gridded rainfall product for Indian subcontinent over the period 1951–2014 [*Pai et al.*, 2015], prepared and extended to the 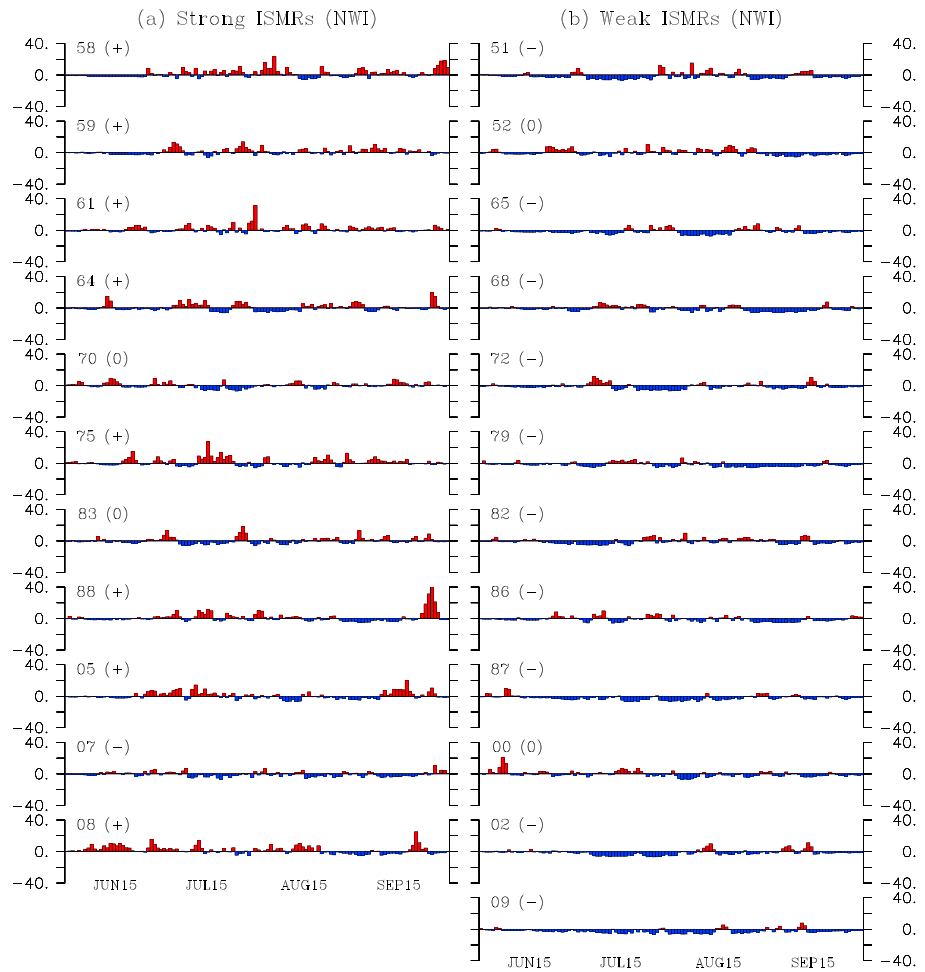latest year by the IMD (the rainfall time series can be found at http://www.imd.gov.in/pages/monsoon_main.php?adta=TS&adtb=India_Daily:). This rainfall product was deemed to be of high quality and well suited to the purposes of the proposed study. First, the daily mean rainfall can be used to analyze the rainfall intensity at short time scales such as synoptic and subseasonal time scales in ways that weekly and monthly rainfall products are not quite suitable. Additionally, this product allows for examination of the rainfall intensity at short time scales (e.g., approximately several days) over each region separately by projecting IMD's four regions onto the daily gridded rainfall grids. The IMD also provides seasonal (JJAS) rainfall series for the four regions over the period 1901–2013. While these seasonal rainfall series are useful for analysis of variability on interannual and decadal time scales, they are not useful for investigation of rainfall variability on shorter time scales (e.g., several days to several weeks), which is the focus of the present study. Therefore, in this particular study we used daily rainfall product instead.

The gridded satellite (GridSat) IR channel (near 11 μm) brightness temperature (T_b) data set is used to capture the regional convective activity and its association with regional rainfall features over each of the chosen regions. The GridSat data set was derived from the International Satellite Cloud Climatology Project (ISCCP) B1 data archive, which is detailed by *Knapp* [2008]. The GridSat data are gridded on a 0.07° latitude equal-angel grid. Satellites are merged by selecting the nadir-most observations for each grid point. The data are derived from full-disk images whose scans are closest to the synoptic times 0000, 0300, …, 2100 UTC each day, which covers the period from 1981 to 2009. In this study, we primarily selected the images at synoptic time 0009Z each day that are available to fully cover the entire Indian subcontinent. A small number of images at 0006Z are used in those cases where the images at 0009Z are not available. Limited by data availability over Indian subcontinent, this approach is useful to roughly represent the convective activity each day.

2.2. Definition of the Strength of ISMRs

In this study, a strong (weak) ISMR year is defined when the total all-India JJAS rainfall for the particular year is more (less) than 10% of the all-India mean JJAS rainfall averaged over the reference period 1951–2014 (i.e., 938 mm). This definition is consistent with the IMD-defined category "excess" ("deficient") of rainfall years (http://pib.nic.in/newsite/PrintRelease.aspx?relid=104920). Hereafter, we refer to these categories as strong and weak years. A nonextreme ISMR year is defined as a year when the departure of the total all-India JJAS rainfall for the year from the long-term mean value is within −10% and 10% of the mean value. We refer to these as normal years acknowledging that there is important variability within this category. In fact, the interannual variation of ISMR has a standard deviation of about 10% of the mean [*Gadgil*, 2003]. In this study, we are more interested in identifying rainfall events when the rainfall departs substantially above (>110%) or below (<90%) the long-term seasonal mean, because excess or deficient rainfall events have a much more

Figure 3. The temporal evolution of daily area-averaged (mm per $1° \times 1°$ grid box) rainfall departure from its corresponding daily climatology over NWI during each strong and each weak ISMR year, which is denoted by the number on the top left of each panel. The signs "plus," "minus," and "zero" in the parentheses denote regional strong, weak, and normal rainfall, respectively. The definition of regional rainfall strength is the same as that of the strength of ISMR for the entire India subcontinent, except that it is applied to each homogeneous rainfall zone (see text in section 3). Periods in red (blue) bars represent the wet (dry) spells of ISMRs, respectively.

severe impact on human life and socioeconomic well-being. Figure 1 shows the evolution of all-India JJAS rainfall over the period 1951–2014 with strong, weak, and normal monsoon years identified according to the above definitions. The rainfall in strong, weak, and normal monsoon years is denoted by red, blue, and gray bars, respectively. During 1951–2014, there are 11 strong monsoon years, 12 weak monsoon years, and 41 normal monsoon years. The years of strong and weak monsoons are denoted at the top of the bars in the figure: the strong ISMR years are 1958, 1959, 1961, 1964, 1970, 1975, 1983, 1988, 2005, 2007, and 2008; and the weak ISMR years are 1951, 1952, 1965, 1968, 1972, 1979, 1982, 1986, 1987, 2000, 2002, and 2009. Clearly, normal rainfall occurs in ~65% of the years (i.e., 41 out of 64 years), although India experienced frequent regional floods and droughts that can be inconsistent with the all-India seasonally averaged rainfall. Given the rainfall variability in space and time, it is expected that some parts of the country get excess rainfall causing floods while other sectors encounter serious deficiency and experience droughts even during normal monsoons. Similarly, where one month gets heavy rainfall, another month may experience break monsoon even during normal monsoons.

The map of daily gridded rainfall can be projected only approximately onto the four IMD regions due primarily to the challenge of exactly delineating the complex boundary between meteorological subdivisions by $1° \times 1°$ grid box. Figure 2 is the projected map of the four regions in the daily rainfall grids: NWI, CI, NEI, and SPIN, which
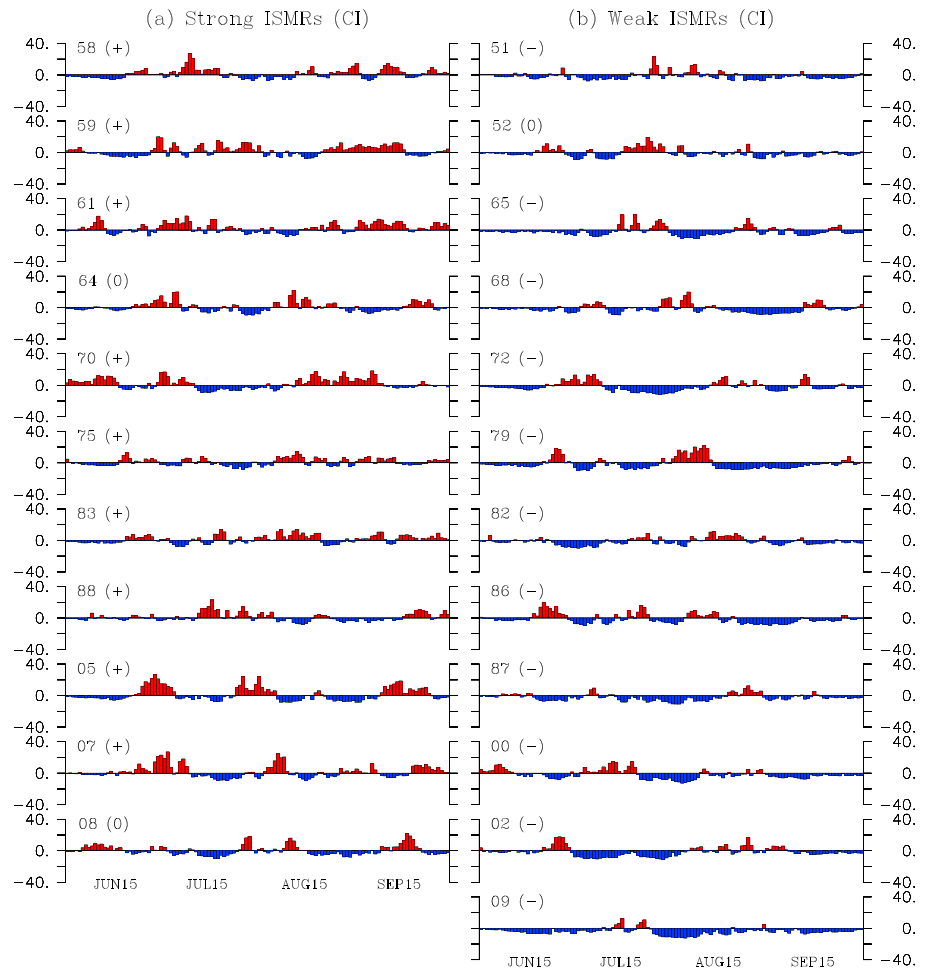
Figure 4. The same as Figure 3 except for CI.

are shown in red, green, orange, and purple, respectively. The daily rainfall is averaged over the grid boxes which encompass the four regions to approximately represent the actual rainfall in those regions.

3. Wet and Dry Spells Between Strong and Weak ISMRs

Rainfall over the four IMD regions may behave differently during a strong or weak ISMR period. Thus, here we first examine the strength of rainfall over each of the four regions during the summer months when an ISMR is strong or weak. The strength of rainfall over each region is referred to as regional strength, and hereafter in this study, is further identified as regional strong, regional weak, or regional normal. The definition of regional strength is the same as that of the ISMR except that it corresponds to the respective IMD region. The temporal variation of daily rainfall anomalies over each region during strong and weak ISMRs has been investigated separately. The daily rainfall anomaly has been computed with respect to the daily climatology over the period 1951–2014. A positive (negative) rainfall anomaly represents an above normal (below normal) condition, respectively. The extended periods of above normal (below normal) conditions represent wet (dry) spells, the features of which are essential to the rainfall strength. Figures 3–6 show the variation of daily rainfall anomalies over NWI, CI, SPIN, and NEI, respectively. The signs plus, minus, and zero in parentheses denote regional strong, regional weak, and regional normal, respectively. Extended wet spells can be considered representative of periods when a monsoon was vigorous or active, while the dry spells represent epochs when a monsoon interrupted the active phase.

Rainfall strength over the NWI region is shown to be consistent with the total ISMR strength (Figure 3). There are eight regional strong rainfall years among the 11 strong ISMR years (8/11, i.e., 73%) and there are 10 regional
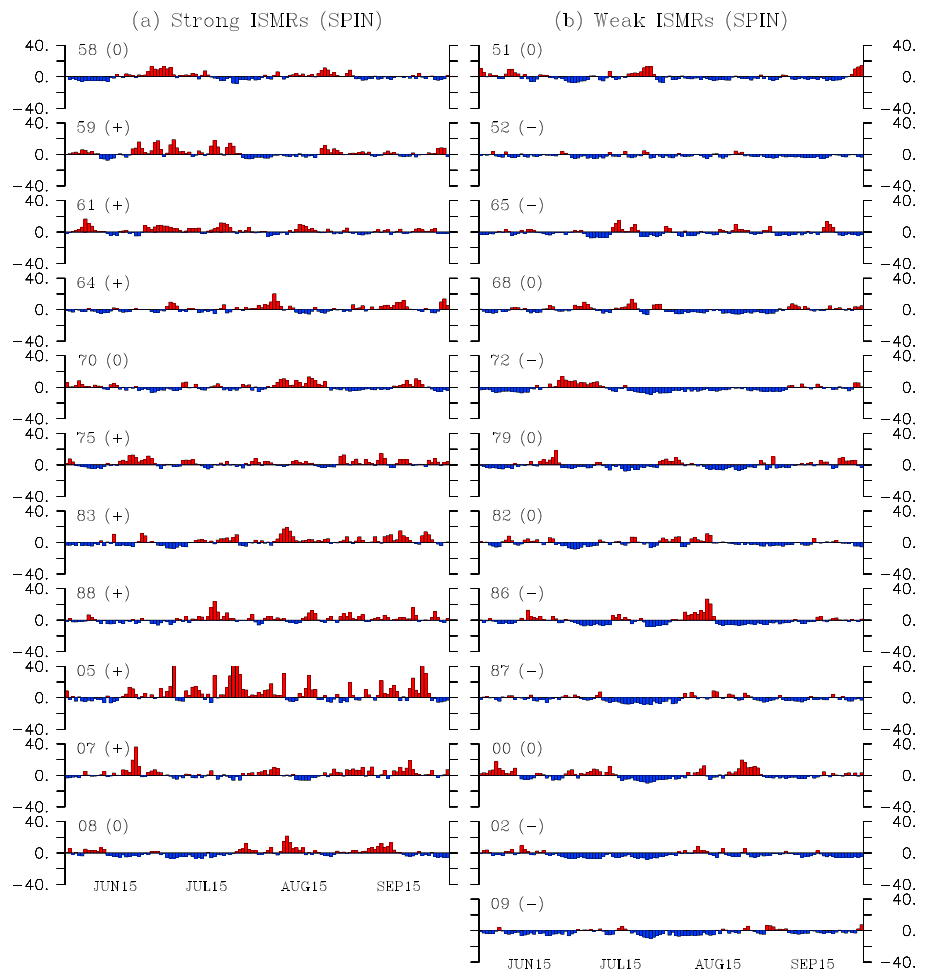
Figure 5. The same as Figure 3 except for SPIN.

weak rainfall years among the 12 weak ISMR years (10/12, i.e., 83%). It is evident that during the regional strong rainfall periods the large amount of rainfall over NWI is partly caused by the relatively intense rainfall for a prolonged period from late June through early July, compared to a moderate-intensity rainfall deficit in late August. Interestingly, the strongest rainfall occurs during late September (the withdrawal phase of ISMR) in several of the regional strong rainfall years (e.g., 1958, 1964, and 1988). This is likely due to the energetic convection systems of July–August that continue to propagate northwestward toward NWI. These convection systems are still vigorous in September of some special years although the monsoon systems overall degenerated. Afterward, there is a reverse propagation of monsoon rainfall moving from the northwest to the southeast, generally beginning in October [e.g., *Janowiak and Xie* 2003]. The weak rainfall over the NWI region during the regional weak years is generally caused by a persistent dry spell followed by a short and small wet spell. The dry spells occur mostly during the mature monsoon phase (July–August).

Over the CI region, the regional rainfall strength is also shown to be synchronous with the ISMR strength (Figure 4). There are nine regional strong rainfall years among the 11 strong ISMR years (9/11, i.e., 82%) and 11 regional weak rainfall years among the 12 weak ISMR years (11/12, i.e., 92%). This implies that the rainfall strength over the CI region can represent the ISMR strength quite well. The large amount of rainfall over the CI region during the regional strong rainfall periods is produced not only by the intensity of rainfall but also by the length of wet spells. The strong rainfall over the CI region can occur during any monsoon phase, while the weak rainfall over this region during the regional weak rainfall periods is largely due to a short active wet spell followed by a prolonged period of dry spell. Generally, the magnitude of rainfall strength fluctuation (−10 to +30 mm/d) during wet and dry spells over the CI region is larger overall than that (−5 to +20 mm/d) which occurs over the NWI region.
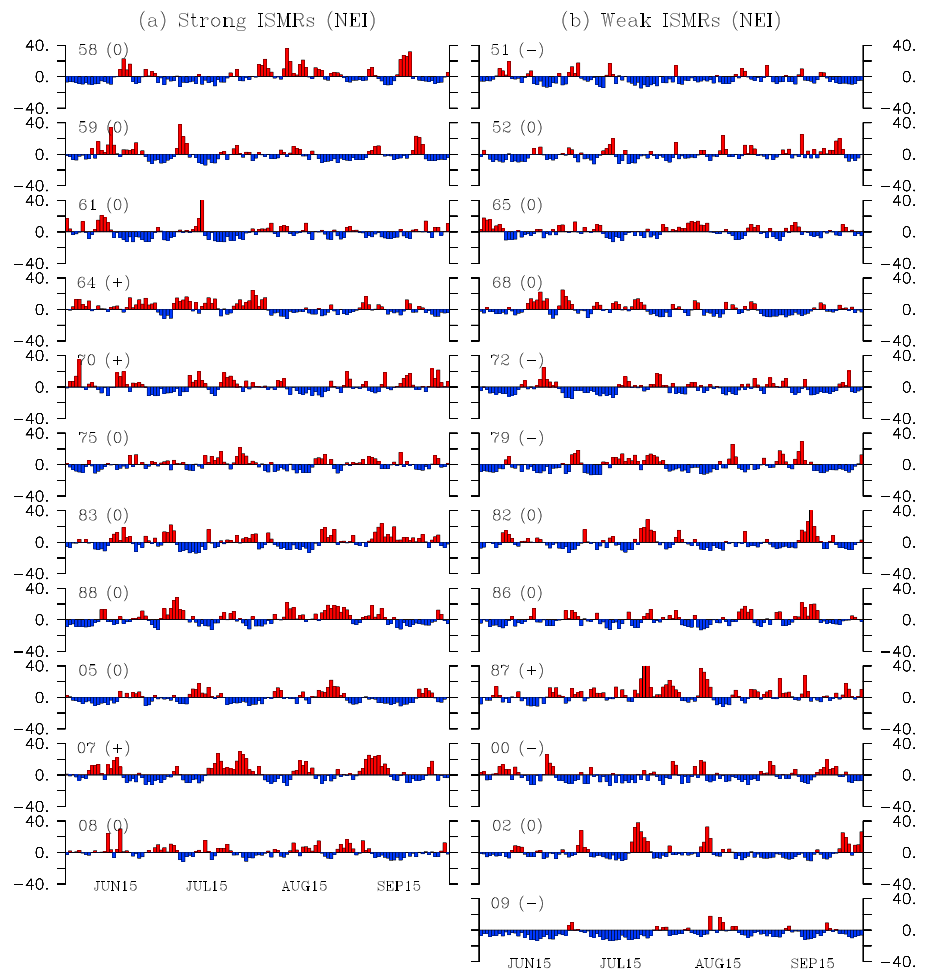
Figure 6. The same as Figure 3 except for NEI.

The strong rainfall over the SPIN region during strong ISMR years is mainly the result of the large amount of rainfall resulting from a long and continuous wet spell followed by the small amount of rainfall seen during a short dry spell (Figure 5). Particularly in 2005, the wet spells of strong rainfall prevailed throughout the summer monsoon period. The characterization for regionally weak rainfall over the SPIN region during weak ISMR years is similar to that of the CI and NWI regions, in that a prolonged and continuous dry spell dominates the entire summer season. The regional strength of rainfall over SPIN is to some degree consistent with the strength of the ISMR; i.e., there exists a 73% (8/11) probability of regional strong rainfall when ISMRs are strong, and there is a 58% probability of regional weak rainfall when ISMRs are weak.

The variation of rainfall is quite different over the NEI region (Figure 6) when compared to the other three regions. First, the strongest fluctuation magnitude of rainfall exists over the NEI region. Second, the regional

Table 1. Conditional Probability (in %) of Rainfall Strength in the Four Homogeneous Regions During Strong ISMRs[a]

Regions	Regional Strong	Regional Weak	Regional Normal
NWI	73%	9%	18%
NEI	27%	0	73%
CI	82%	0	18%
SPIN	73%	0	27%

[a]Regional rainfall strength is categorized into regional strong, regional weak, and regional normal, which are defined as the departure of regional rainfall from its seasonal mean in the corresponding region by more than 10%, less than −10%, and within −10% and +10%, respectively. The results are based on the daily gridded data sets over the period 1951–2014.

Table 2. The Same as Table 1 Except for Weak ISMRs

Regions	Regional Strong	Regional Weak	Regional Normal
NWI	0	83%	17%
NEI	8%	42%	50%
CI	0	92%	8%
SPIN	0	58%	42%

strength of rainfall over the NEI region appears to have no clear linkage to the strength of an ISMR. For example, there is only a 27% (i.e., 3/11) probability of regional strong rainfall over the NEI region when ISMRs are strong, and there is only a 42% (i.e., 5/12) probability of regional weak rainfall when ISMRs are weak. It is clear that regional normal rainfall dominates over the NEI region when ISMRs are either strong or weak. Thus, we speculate that mechanisms controlling the rainfall strength of this region may be different from those over other three regions. While this idea should be further investigated, it is beyond the scope of this observation-based study. As discussed in a study by *Zheng et al.* [2016] in which the mean JJAS rainfall values for the four homogeneous regions directly provided by IMD were used, it is difficult to keep track of the strength of an ISMR (strong or weak) through the identification of rainfall strength over the NEI region, although the rainfall has the greatest magnitude among the four regions. The result in the present study is consistent with the *Zheng et al.* [2016] study.

The conditional probability of rainfall strength in the four homogeneous regions is summarized in Tables 1–3. These tables clearly show that rainfall strength over the NWI, CI, and SPIN regions predominantly evinces the strength of an ISMR over the entire Indian subcontinent.

4. Association of Regional Strength With ISMR Strength

To further illustrate the association of regional rainfall strength with the strength of ISMR, we present a scatterplot of JJAS rainfall over the four homogeneous regions versus the ISMR (Figure 7). The Pearson correlation coefficient computed for each region is provided in the upper right corner of each panel. It is evident that the variations in ISMR are highly correlated with the rainfall variations over CI with a positive correlation coefficient of 0.87, followed by rainfall variations over NWI with a correlation coefficient of 0.81, and rainfall variations over SPIN with a correlation coefficient of 0.73. These correlations of ISMR with rainfall variations over CI, NWI, and SPIN are all statistically significant at a 99% confidence level. By contrast, the linkage of rainfall variation over NEI with that of ISMR variation appears much weaker with a correlation coefficient of only 0.31, which is not statistically significant at a 99% confidence level.

The fact that the relationship between rainfall over NEI and ISMR is much weaker than those over the other three regions implies that the mechanisms controlling the rainfall over NEI is different than those in the other three regions. For example, most portions of NWI and CI are located within the so-called monsoon zone [*Sikka and Gadgil*, 1980], which is a broad zone approximately 20°N and stretching northwestward from the head of the Bay of Bengal. During the summer monsoon season, the rainfall events over CI and NWI are closely associated with the northwestward propagation of a series of organized convective systems on synoptic and supersynoptic scales. These systems are generated over the Bay of Bengal and move onto the Indian subcontinent. Over SPIN, high precipitation usually occurs along the west coast of the peninsula due to orographic lifting effects and to a large amount of moisture transported by the low-level tropospheric southwest winds from the Arabian Sea. Therefore, the rainfall over CI, NWI, and SPIN is closely tied to these well-known features of ISMRs. However, the features of rainfall over NEI appear to be different from the other three regions, which leads us to postulate that the rainfall behaviors over NEI either has no close association with these common

Table 3. The Same as Table 1 Except for Normal ISMRs

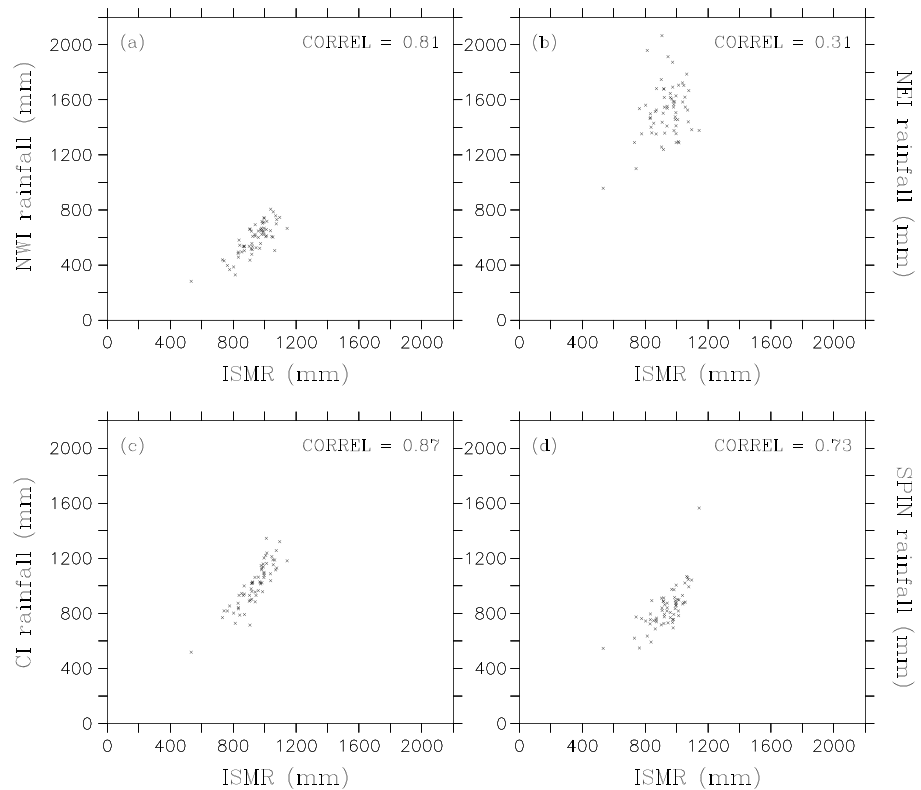| Regions	Regional Strong	Regional Weak	Regional Normal
NWI	39%	20%	41%
NEI	22%	20%	58%
CI	24%	15%	61%
SPIN	7%	22%	71%

Figure 7. Scatter plot of regional JJAS rainfall versus total ISMR for (a) NWI, (b) NEI, (c) CI, and (d) SPIN. Correlation coefficient is included on the top right corner of each panel. Correlation between regional rainfall and total ISMR is significant at a 99% confidence level for NWI, CI, and SPIN.

summer monsoon features or the local variability is so great that much denser precipitation observations would be needed to reduce the uncertainty in the regional average.

5. Probability Density Function (PDF) Distribution of Daily Rainfall

We will show the salient features of daily rainfall PDF distribution over the four regions for each month and the entire summer monsoon season between different categories of ISMRs. A PDF analysis of the daily rainfall allows us to characterize notable differences in rainfall events between NEI and the other three regions. We first display the PDF distribution of daily rainfall in NWI (Figure 8). The unit of abscissa is millimeter per unit grid box ($1^o \times 1^o$) and the unit of the y coordinate is the count percentage demonstrating the probability of occurrence per unit y axis. Integrating over the axis results in the probability of daily rainfall events, being between daily rainfalls used for bounds of integration. The PDFs are used because they are relatively insensitive to gaps in the observation records, allowing for comparison between geographical regions with differing amounts of input. The PDFs are determined by dividing the count in each rainfall bin by the total days of rainfall and by the bin width. The PDFs address only the difference of characteristics on days that rain occurs. The number of rain days, discussed above, is also an important consideration.

Over NWI, a common feature related to PDF distribution of daily rainfall during June–September is that the lower the rainfall intensity, the more frequently it occurs during strong, weak, and normal ISMR years. The major differences exist in low-intensity (0–5 mm) and moderate-intensity (6–10 mm) rainfalls between strong and weak ISMR years; i.e., low-intensity rainfalls occur much more frequently during weak ISMR years while moderate-intensity rainfalls occur more frequently during strong ISMR years. A difference can also be seen in each month for strong, weak, and normal ISMR years, most obviously in September. This is likely due to the variations of the tropical convergence zone (TCZ) and northward propagating systems that occur frequently over NWI in September. Another interesting feature is that extreme daily rainfalls occur occasionally (>15 mm) during strong ISMR years; while such extreme rainfalls are almost nonexistent during
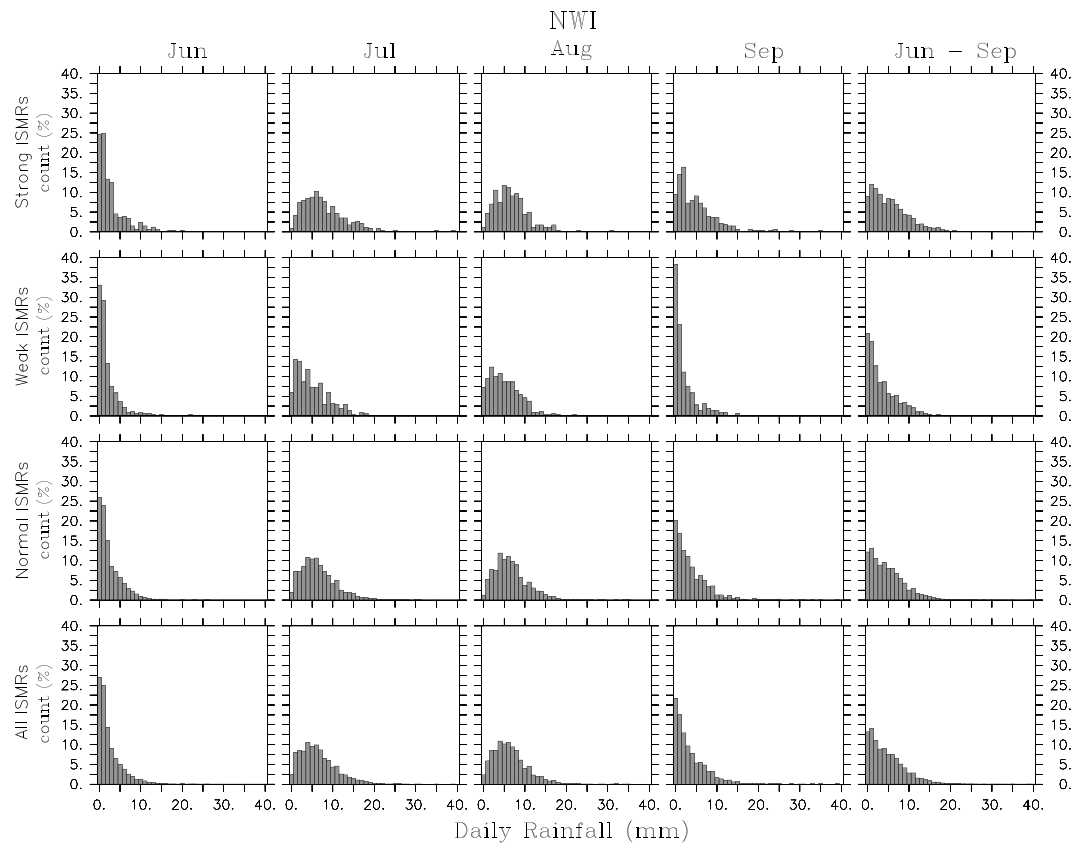
Figure 8. PDF distribution of daily rainfall over NWI during strong, weak, normal ISMR years, and across all years (1951–2014). All counts are normalized to 100 for comparison purposes among the months of each ISMR category over different regions, so that the integration of the y values over the x axis represents the occurring probability (in %) for each rainfall range.

weakISMR years. However, it should be noted that although such extreme rainfalls occur infrequently (about 1–2%) during strong ISMR years, they do contribute to the enhanced rainfall over NWI. The PDF distribution during normal ISMR years is quite similar to that during all 64 years. Furthermore, the rainfall range over NWI appears narrow (i.e., within 0–20 mm). In addition to occasional extreme rainfall events during strong ISMR years, there are more frequent moderate-intensity rainfalls (6–10 mm) (about 5–8%) during strong ISMR years than those (~2–5%) during weak ISMR years in this region. The combination of these factors contributes to the differences of rainfall over NWI between strong and weak ISMR years.

Hypothetically, these differences in precipitation rate can have a very large impact on water resources. Light rains tend to be evaporated before the rainwater sinks far into the soil, and there is little runoff. Moderate rain can penetrate much further into the soil, which is important for agriculture, and the runoff can be captured.

Over the CI region, the profile of PDF distribution between strong and weak ISMR years is more distinguishable (Figure 9), which results in significant differences in rainfall intensity. It is evident that the PDF distribution differs during each month of summer monsoon season between strong and weak ISMR years. Overall, for June through September there are more frequent rainfalls of 10–20 mm during strong ISMR years than during weak ISMR years. In contrast, low-intensity (i.e., 0–5 mm) rainfall occurs more frequently (5%–13%) during weak ISRM years, primarily in July and September, than (<5%) during strong ISMR years. As a result, during weak ISMR years, the higher the rainfall intensity, the less frequently it occurs. Although during strong ISMR years the peak frequency spectrum (~5%) of moderate-intensity rainfalls (5–10 mm) bears a resemblance to that during weak ISMR years, it is the high-intensity rainfalls (>10 mm) that decline more slowly during strong ISMR years than those occurring during weak ISMR years, giving rise to strong rainfall in this region. Again, the PDF distribution in normal ISMR years is quite similar to that of all years during the period 1951–2014 since normal ISMR years occupy 64% (i.e., 41/64) of the 64 years. It should be noted that rainfall
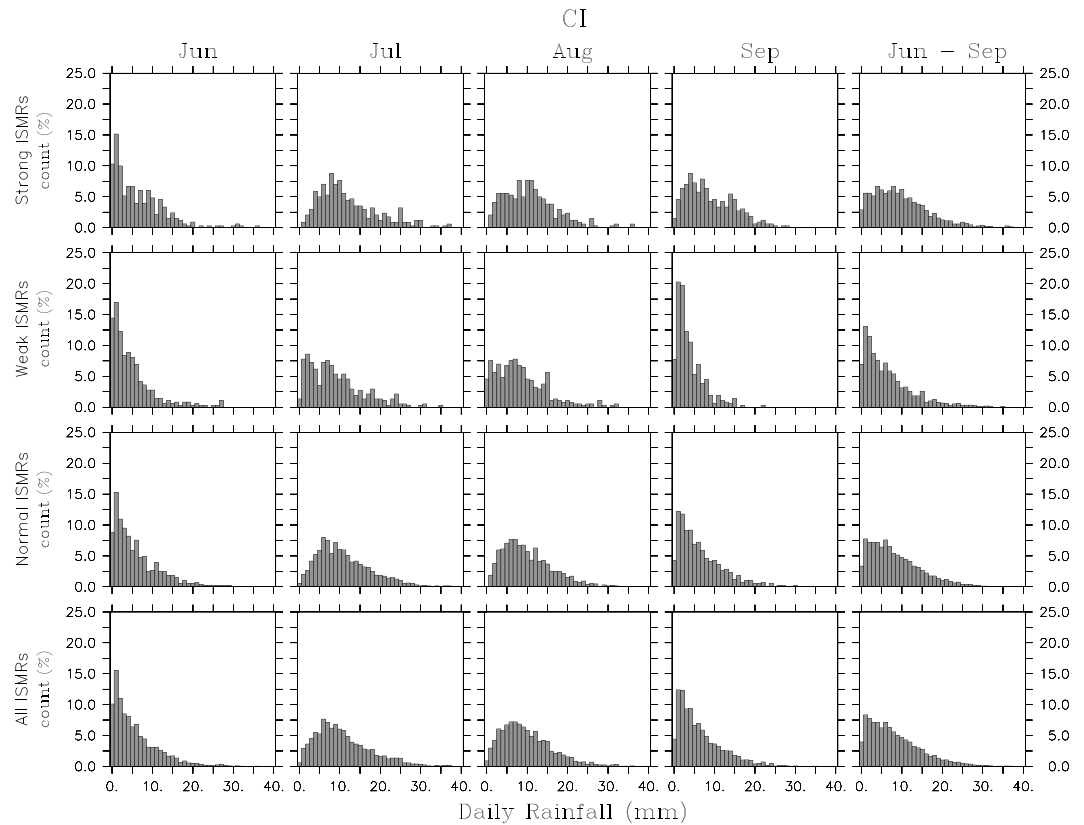
Figure 9. The same as Figure 8 except for CI.

intensity over CI has a broader range (0–30 mm) than that (0–20 mm) over NWI. In all likelihood, this occurs due to the difference in spatial configuration of moisture supply during summer monsoon season; i.e., the moisture transported by the prevalent southwest winds from the Arabian Sea across CI is more than that across NWI. However, the difference could simply be related to greater convergence in rainier regions.

Over the SPIN region, the PDF distribution between strong and weak ISMR years differs remarkably each month and thus over the entire monsoon period (Figure 10). For example, rainfalls of 5–10 mm occur prevalently in the frequencies greater than 7.5% during June–September of strong ISMR years, while rainfalls of 2–7 mm occur prevalently in the frequencies larger than 7.5% during June–September of weak ISMR years. Meanwhile, during the strong ISMR years the high-intensity rainfalls (>10 mm) occur more frequently than during the weak ISMR years and extreme rainfalls (>20 mm) occur more often during the strong ISMR years. These results can clearly be seen in the distinctive PDF distribution between strong and weak ISMRs for each month. In particular, rainfalls of moderate to high intensity (>5 mm) occur more frequently for July, August, and September during strong ISMRs than during weak ISMRs. Again, the PDF profile for normal ISMRs is quite similar to that for all ISMRs.

The discrepancies in PDF distribution over NEI between strong and weak ISMRs are not discernible (Figure 11), in comparison to the other three regions. This suggests that the rainfall variations over the NEI region have no clear connection to the strength of ISMRs and/or that the local variability is very large compared to the ISMR signal. The resemblance of daily rainfall PDF distribution among strong, weak, and normal ISMRs explains why the rainfall in NEI is predominantly normal whether an ISMR is strong, weak, or normal (see Tables 1–3). As illustrated in Figures 3–7, the rainfall over NEI appears the largest relative to that over the other three rainfall zones. Consequently, the rainfall over NEI has the broadest range (0–40 mm) compared to the rainfall ranges over the other three regions. In summary, rainfall behaviors over NEI are remarkably different from those over the other three regions, which leads us to hypothesize that the mechanisms controlling rainfall over NEI are likely independent of mechanisms that generally control the strength of ISMRs.
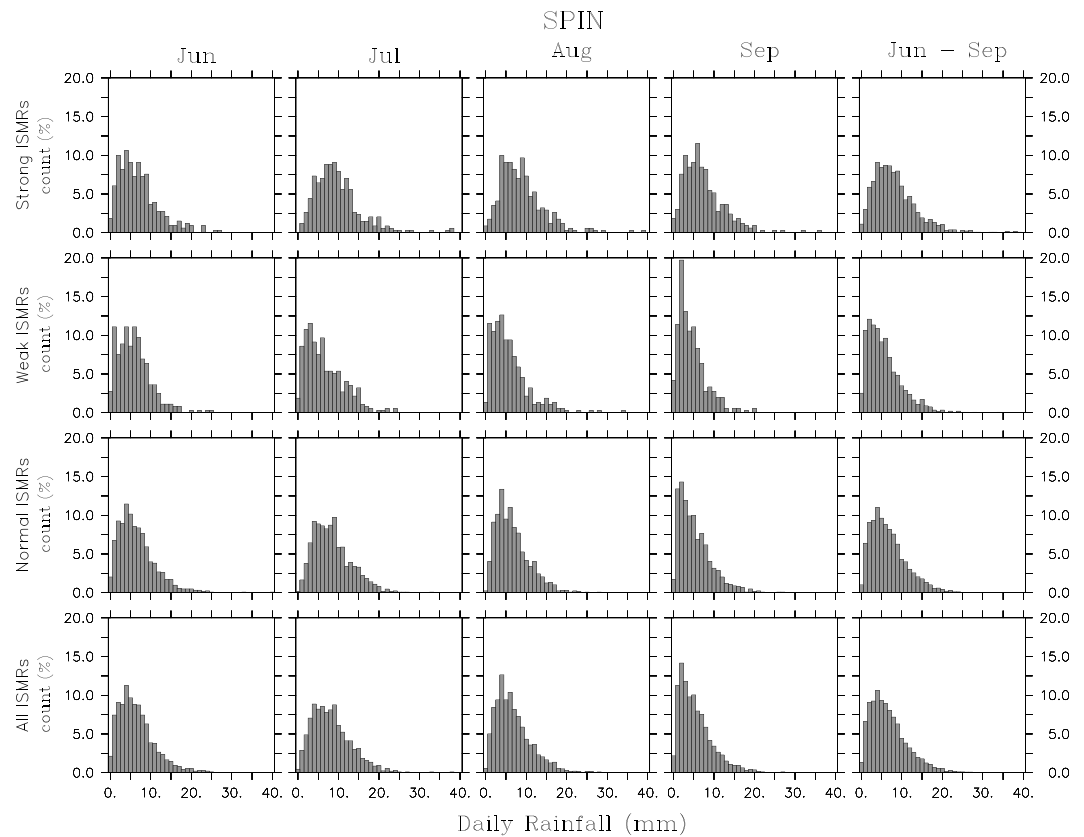
Figure 10. The same as Figure 8 except for SPIN.

6. Discussions

The mechanisms for the regionally distinct features of rainfall rate over NEI have yet to be clearly unraveled. Since NEI is adjacent to Bangladesh, it is reasonable to argue that the physical processes for rainfall features over NEI may be similar to those for rainfall over Bangladesh. For example, the average summer monsoon rainfall over Bangladesh is neither related to El Niño Southern Oscillation (ENSO) nor the equatorial Indian Ocean Oscillation (EQUINOO) [*Gadgil et al.*, 2011], while the physical processes associated with ENSO and EQUINOO play a role in determining the ISMR [*Gadgil et al.*, 2004; *Ihara et al.*, 2007]. The differences in summer monsoon rainfall over NEI and other parts of India are also likely to be caused by the Asian summer monsoon onset processes. For example, an observational study [*Liu et al.*, 2015] showed that after the Asian summer monsoon commences over the eastern Bay of Bengal around early May, the monsoon onset can propagate eastward toward the South China Sea and the west Pacific; however, its westward propagation to the Indian subcontinent can be blocked. They further pointed out that such blocking is caused by the change in both large-scale circulation and air-sea interaction due to the monsoon onset over the Bay of Bengal. In addition, abundant moisture over the Arabian Sea is transported by the prevailing southwest winds to Indian subcontinent during summer monsoon seasons. The supply of moisture from the Arabian Sea is critically important to the development of a series of northwestward convection systems over the Indian subcontinent that are initiated in the Bay of Bengal. It is well known that the evolution and development of these convection systems play an important role in Indian summer monsoon rainfall. However, the above fundamental rainfall-triggering processes for Indian summer rainfall may have less influence on the rainfall over NEI region than on rainfall over other regions of the Indian subcontinent because NEI is the farthest location from the moisture source and not in the prevailing track of northwestward convection systems.

Here we postulate that the distinctive features of daily convective activity over different regions may play an important role in determining the salient daily rainfall features over these regions during strong
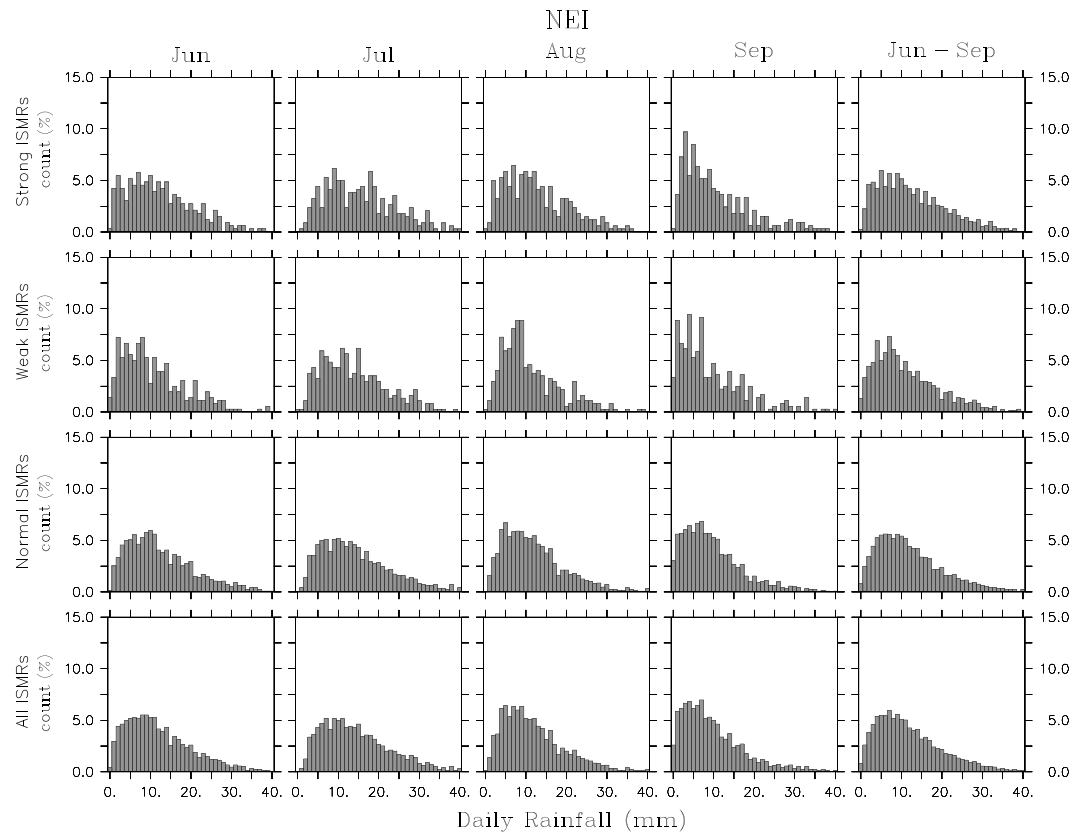
Figure 11. The same as Figure 8 except for NEI.

and weak monsoons. Noting that the GridSat covers only the period 1981–2009, any analysis of brightness temperature (T_b, unit: Kelvin) during strong and monsoons is limited to these periods based on data availability. We first examine the PDF of T_b between strong and weak monsoons. Figure 12 shows the PDF of T_b averaged over NWI, NEI, CI, and SPIN between strong, weak, and normal monsoons, and all entire periods (i.e., 1981–2009). Emphasis is placed upon the distinctive features of T_b between strong and weak monsoons. Generally speaking, the lower the T_b, the colder the cloud tops and the stronger the convective activity. Overall, lower T_b occurs more frequently during strong monsoons versus during weak monsoons except over NEI where the disparity in PDFs is not easily distinguishable. Similarly, overall higher T_b occurs more frequently during weak monsoons versus strong monsoons, again except over NEI. The results suggest that strong convective processes tend to occur more frequently during strong monsoons than they do during weak monsoons except over NEI. The discrepancies in the frequency of occurrence of strong convective activity within a day over NWI, CI, and SPIN between strong and weak monsoons may help interpret the differences of the daily rainfall over these regions between strong and weak monsoons.

To further understand whether the vitality of convective activity is closely linked to the strength of daily rainfall over each region, we present a scatterplot of T_b versus the daily rainfall over each region (Figure 13). The Pearson correlation coefficient computed for each region is provided in the top right corner of each panel. It is evident that the variations in daily rainfall are highly correlated with the T_b variations over CI with a correlation coefficient of −0.66, followed by T_b variations over NWI with a correlation coefficient of −0.62, T_b variations over NEI with a coefficient of -−0.51, and T_b variations over SPIN with a coefficient of −0.46. The negative sign of correlation coefficient indicates that the lower T_b, the stronger the convective activity, which tends to give rise to stronger rainfall. These correlations between rainfall and T_b variations over the four regions are statistically significant at a 99% confidence level. The spatial distribution for T_b versus daily rainfall rate over NEI (Figure 13b)
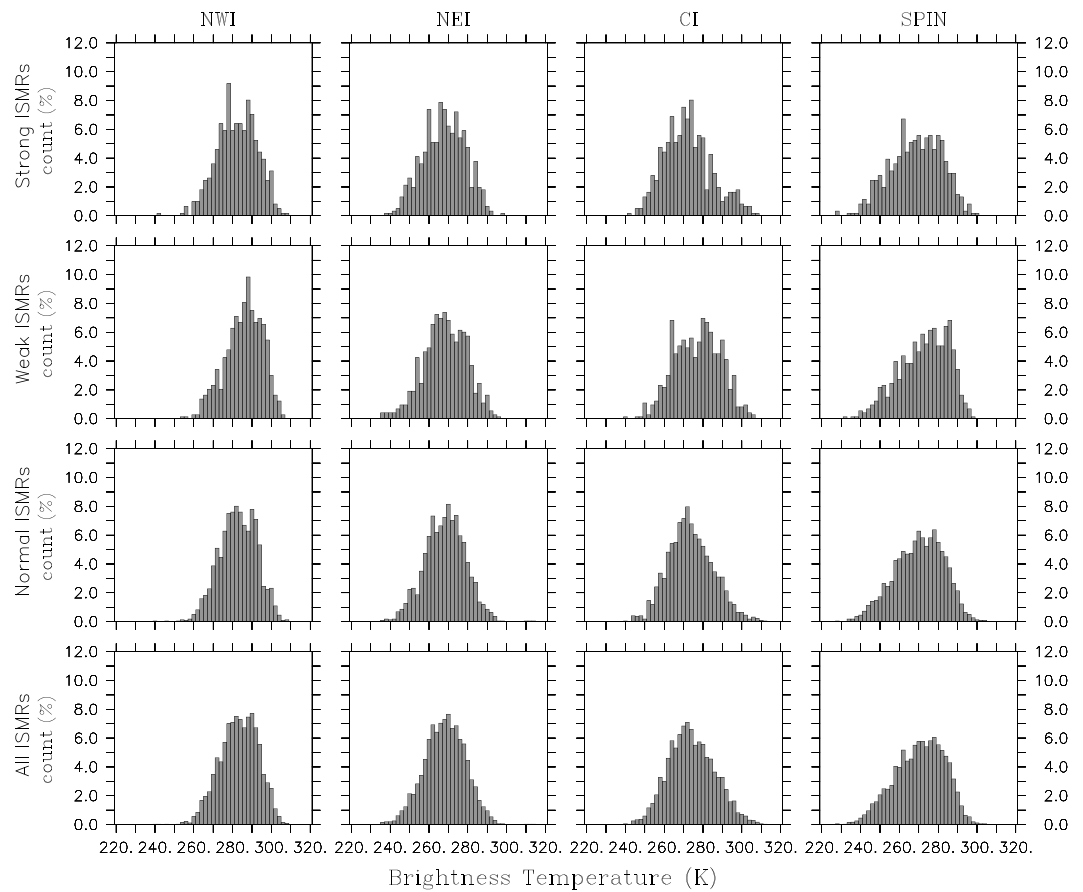
Figure 12. PDF distribution of brightness temperature (T_b) over NWI, NEI, CI, and SPIN during strong, weak, normal ISMR years, and across all years (1981–2009). All counts are normalized to 100 for comparison purposes among the months of each ISMR category over different regions, so that the integration of the y values over the x axis represents the occurring probability (in %) for each T_b range.

appears more scattered than that over NWI, CI, and SPIN (Figures 13a, 13c, and 13d), implying that larger uncertainty exists between daily rainfall and convective activity over NEI. It is notable that the PDFs in T_b, as well as in daily rainfall rate over NEI between strong and weak monsoons are physically consistent. Also, note that the T_b features shown here are on a daily basis and they can represent the convective activity on small time scales (e.g., synoptic, intraseasonal time scales). The convective activity on such time scales is associated with the northward propagation of Madden-Julian Oscillation (MJO) during Indian summer monsoon seasons; thus, we speculate that these rainfall features found in this study may be associated with the northward propagation of MJO initiating over Indian Ocean. Better understanding this important aspect is beyond the scope of this study; however, it will be examined in future studies.

From the perspective of atmospheric dynamics and thermodynamics, there are many factors that can give rise to the distinct characteristics of rainfall over NEI compared to rainfall over the other three Indian homogeneous regions. These factors include, but are not limited to, differences in (1) atmospheric stratification; (2) wind speed enhancing or diminishing moisture advection from the sea, which would also modify evaporation and stratification; (3) available moisture for sustaining convection; (4) cloud cover modifying the diurnal cycle and modifying afternoon convection; and (5) changes in the strength of northward propagating disturbances associated with TCZ and/or MJO. It will be useful to investigate these aspects between strong and weak monsoons over different regions to better understand the potential mechanisms responsible for the differences of Indian summer monsoon rainfall identified in this study.
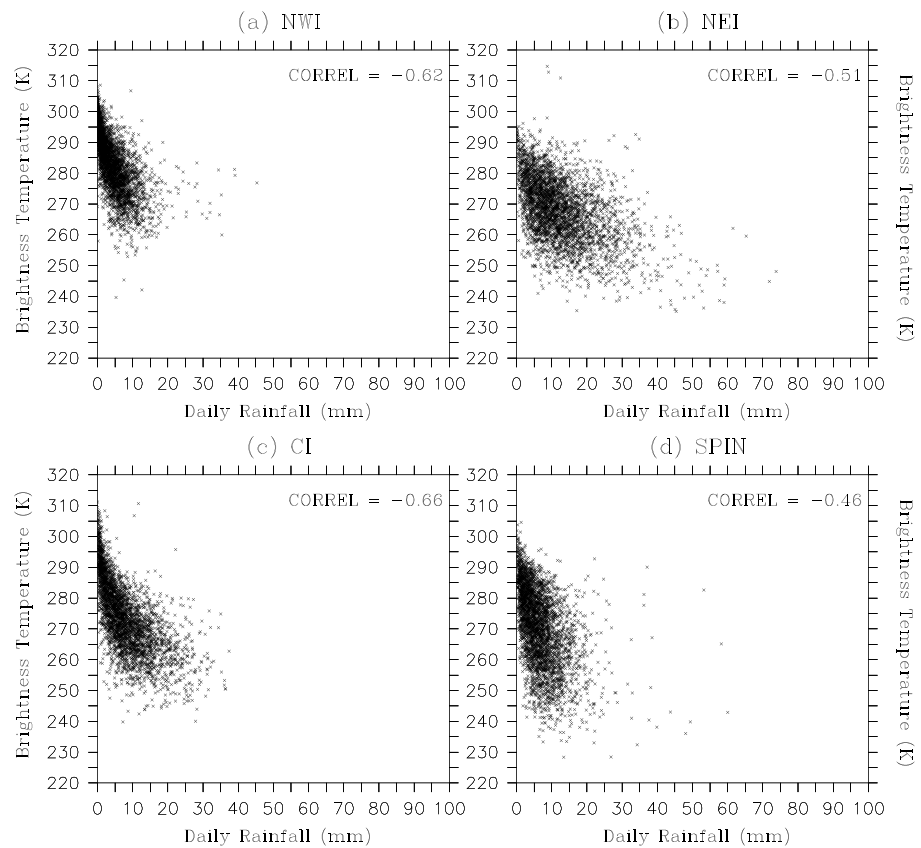
Figure 13. Scatter plot of brightness temperature (T_b) versus daily rainfall for (a) NWI, (b) NEI, (c) CI, and (d) SPIN. Correlation coefficient is included on the top right corner of each panel. Correlation between regional rainfall and total ISMR is significant at a 99% confidence level for NWI, NEI, CI, and SPIN.

7. Summary and Conclusions

In this study, salient features of rainfall behaviors over India's four homogeneous regions during strong, weak, and normal ISMR years, with particular focus on the strong and weak monsoons, are investigated using the most recent daily gridded rainfall data set prepared by the IMD for the period 1951–2014.

The variation of anomalous daily rainfall over the four homogeneous regions (Figures 3–6) reveals the features of deficit and excess rainfall during strong and weak ISMR years. It is evident that rainfalls over NWI, CI, and SPIN are primarily strong (weak) during strong (weak) ISMR years. The strong rainfall over NWI, CI, and SPIN during the strong monsoons is generally caused by the prolonged (~1–3 weeks) and strong wet spells followed by short and/or weak dry spells, primarily during the mature phase (July–August) and the withdrawal phase (September). Similarly, the weak rainfall over NWI, CI, and SPIN during the weak monsoons is largely caused by the prolonged (~2–3 weeks) and strong dry spells mainly during the mature phase, followed by short wet spells (approximately several days to 1 week). The behavior of rainfall over NEI has no clear distinction between the strong and weak ISMR years. In fact, the fluctuation of excess rainfall over NEI tends to be similar to that of deficit rainfall regarding strength and duration between the strong and weak ISMR years. As a result, a majority of normal rainfall dominates over this region during June–September. Tables 1–3 summarize the results regarding the conditional probability of regional rainfall strength categories over each region. It is important to note that more than 50% of the seasonal mean rainfalls over NEI are within ±10% fluctuation of the region's long-term averaged values regardless of whether an ISMR is strong, weak, or normal.

The correlation analysis (Figure 7) demonstrates that the strength of rainfall over CI, NWI, and SPIN is closely associated with the strength of ISMRs (the correlation coefficient is 0.87, 0.81, and 0.73, respectively), while the strength of rainfall over NEI shows no clear association with the strength of ISMR (the correlation

coefficient is 0.31, which is not statistically significant at a 99% confidence level). The latter suggests that the mechanisms controlling the rainfall over NEI are either different from those controlling the strength of ISMRs or the local variability is not well captured by the rain gauge network. In other words, the prediction skills used for ISMR forecasting may not be applicable to rainfall prediction over the NEI region.

The PDF distribution of daily rainfall over the four regions provides a means of interpreting the above results (Figures 8–11). The strong rainfall over NWI, CI, and SPIN during the strong ISMR years is generally produced by the greater frequencies of high intensity of rainfall (>10 mm/d) and/or moderate intensity (5–10 mm/d), while the weak rainfall over NWI, CI, and SPIN during the weak ISMR years is mainly caused by the much more frequent low-intensity rainfall (<5 mm/d) and relatively low frequency of high-intensity rainfall. The PDF profiles of daily rainfall over NEI are quite similar during strong, weak, and normal ISMR years, indicating that the rainfall over NEI shows no sensitivity to the strength of ISMRs. This insensitivity over NEI can also be found in terms of resemblance of convective activity between strong and weak monsoons (Figure 12), which partly interprets the similar rainfall behaviors over NEI between strong and weak ISMRs. Since the rainfall over the Indian subcontinent is closely linked with the regional convective activity (Figures 12 and 13), we hypothesize that the rainfall features found in this study may be associated with the northward propagation of MJO starting in the Indian Ocean.

References

Annamalai, H., J. Hafner, K. P. Sooraj, and P. Pillai (2013), Global warming shifts the monsoon circulation, drying south Asia, *J. Clim.*, *26*, 2701–2718, doi:10.1175/JCLI-D-12-00208.1.

Dash, S. K., M. S. Shekhar, G. P. Singh, and A. D. Vernekar (2002), Relationship between surface fields over Indian Ocean and monsoon rainfall over homogeneous zones of India, *Mausam*, *53*(2), 133–144.

De, U. S., R. R. Lele, and J. C. Natu (1998), Breaks in southwest monsoon. IMD Rep. 1998/3, 11 pp.

Gadgil, S. (2003), The Indian monsoon and its variability, *Annu. Rev. Earth Planet. Sci.*, *31*, 429–467.

Gadgil, S., Yadumani, and N. V. Joshi (1993), Coherent rainfall zones of the Indian region, *Int. J. Climatol.*, *13*, 547–566.

Gadgil, S., P. N. Vinaychandran, P. A. Francis, and S. Gadgil (2004), Extremes of Indian summer monsoon rainfall, ENSO, equatorial Indian Ocean Oscillation, *Geophys. Res. Lett.*, *31*, L12213, doi:10.1029/2004GL019733.

Gadgil, S., M. N. Rajeevan, L. Zubair, and P. Yadav (2011), Interannual variation of the south Asian monsoon: Links with ENSO and EQUINOO, in *The Global Monsoon System: Research and Forecast*, vol. 5, 2nd ed., edited by C.-P. Chang et al., chap. 3, pp. 25–42, World Scientific.

Goswami, B. N. (2005), Intraseasonal variability (ISV) of south Asian summer monsoon, in *Intraseasonal Variability of the Atmosphere—Ocean Climate System*, edited by K. Lau and D. Waliser, pp. 19–61, Springer, Berlin.

Ihara, C., Y. Kushnir, M. A. Cane, and V. H. De la Pena (2007), Indian summer monsoon rainfall and its link with ENSO and the Indian Ocean climate indices, *Int. J. Climatol.*, *27*, 179–187.

Iyengar, R. N., and P. Basak (1994), Regionalization of Indian monsoon rainfall and long term variability signals, *Int. J. Climatol.*, *14*, 1095–1114.

Janowiak, J. E., and P. Xie (2003), A global—scale examination of monsoon—related precipitation, *J. Clim.*, *16*, 4121–4133.

Knapp, K. R. (2008), Scientific data stewardship of International Satellite Cloud Climatology Project B1 global geostationary observations, *J. Appl. Remote Sens*, *2*, 023548, doi:10.1117/1.3043461.

Kripalani, R. H., and A. Kulkarni (2001), Monsoon rainfall variations and teleconnections over south and east Asia, *Int. J. Climatol.*, *21*, 603–616.

Kripalani, R. H., A. Kulkarni, S. S. Sabade, and M. L. Khandekar (2003), Indian monsoon variability in a global warming scenario, *Nat. Hazards*, *29*, 189–206.

Krishnamurthy, V., and J. Shukla (2000), Intraseasonal and interannual variability of rainfall over India, *J. Clim.*, *13*, 4366–4377.

Kulkarni, A., R. Kriplani, S. Sabade, and M. Rajeevan (2011), Role of intra-seasonal oscillations in modulating Indian summer monsoon rainfall, *Clim. Dyn.*, *36*, 1005–1021, doi:10.1007/s00382-010-0973-1.

Kumar, K. K., B. Rajagopalan, M. Hoerling, G. Bates, and M. Cane (2006), Unraveling the mystery of Indian monsoon failure during El Niño, *Science*, *314*, 115–119, doi:10.1126/science.1131152.

Liu, B., Y. Liu, G. Wu, J. Yan, J. He, and S. Ren (2015), Asian summer monsoon onset barrier and its formation mechanism, *Clim. Dyn.*, *45*, 711–726, doi:10.1007/s00382-014-2296-0.

Malik, N., N. Marwan, and J. Kurths (2010), Spatial structures and directionalities in monsoonal precipitation over South Asia, *Nonlinear Processes Geophys.*, *17*, 371–381.

Nicholson, S. E. (1986), The spatial coherence of African rainfall anomalies: Interhemisphere teleconnections, *J. Climate Appl. Meteorol.*, *25*, 1365–1381.

Pai, D. S., L. Sridhar, and R. Kumar (2015), Active and break events of Indian summer monsoon during 1901–2014, *Clim. Dyn.*, doi:10.1007/s00382-015-2813-9.

Parthasarathy, B., A. A. Munot, and D. R. Kothawale (1992), Indian summer monsoon rainfall indices: 1871–1990, *Meteorol. Mag.*, *121*, 174–186.

Parthasarathy, B., K. Rupakumar, and A. A. Munot (1994), All-India monthly and seasonal rainfall series: 1871–1994, *Theor. Appl. Climatol.*, *49*, 217–224.

Parthasarathy, B., A. A. Munot, and D. R. Kothawale (1995), Monthly and seasonal rainfall series for all-India homogeneous regions and meteorological subdivisions: 1871–1994. *IITM Res. Rep.-065*, Indian Inst. of Trop. Meteorol., Pune, India.

Pattanaik, D. R. (2007a), Analysis of rainfall over different homogeneous regions of India in relation to variability in westward movement frequency of monsoon depressions, *Nat. Hazards*, *40*, 635–646.

Pattanaik, D. R. (2007b), Variability of convective activity over the northern Indian Ocean and its association with monsoon rainfall over India, *Pure Appl. Geophys.*, *164*, 1527–1545.

Rajeevan, M., S. Gadgil, and J. Bhate (2010), Active and break spells of the Indian summer monsoon, *J. Earth Syst. Sci.*, *119*, 229–247.

Ramamurthy, K. (1969), Monsoon of India: Some aspects of the "break"in the Indian southwest monsoon during July and August. India Meteorological Department FMU Rep. IV-18-3, 13 pp.

Rao, T. N., K. N. Uma, T. M. Satyanarayana, and D. N. Rao (2009), Differences in draft core statistics from the wet spell to dry spell over Gandaki, India (13.58°N, 79.28°E), *Mon. Weather Rev.*, *137*, 4293–4306.

Sahai, A. K., D. R. Pattanaik, V. Satyan, and M. G. Alice (2003), Teleconnections in recent time and prediction of Indian summer monsoon rainfall, *Met. Atmos. Phys.*, *84*, 217–227.

Sikka, D. R., and S. Gadgil (1980), On the maximum cloud zone and the ITCZ over India longitude during the southwest monsoon, *Mon. Weather Rev.*, *108*, 1840–1853.

Thapliyal, V., and S. M. Kulshrestha (1991), Climate changes and trends over India, *Mausam*, *42*, 333–338.

Zheng, Y., M. M. Ali, and M. A. Bourassa (2016), Contribution of monthly and regional rainfall to the strength of Indian summer monsoon, *Mon. Weather Rev.*, doi:10.1175/MWR-D-15-0318.1.